Experimental study of droplets in evaporating regime by 2D scattering analysis

by

R. Calabria and P. Massoli

Istituto Motori - CNR

Via Marconi 8, 80125 Napoli, Italy

ABSTRACT

The characterisation of droplets in terms of velocity, size and composition is fundamental in the analysis of several industrial process and natural phenomena. A lot of efforts has hence been made by the scientific community to develop non-intrusive techniques based on the properties of the scattered light. In 1990, Ragucci et al., originally developed a planar sizing technique based on the measurement of the angular spacing between fringes in out-of-focus images. In fact, in out-of-focus images (fig. 1) the scattering intensity oscillations, whose spacing is inversely proportional to droplet size, are clearly visible.
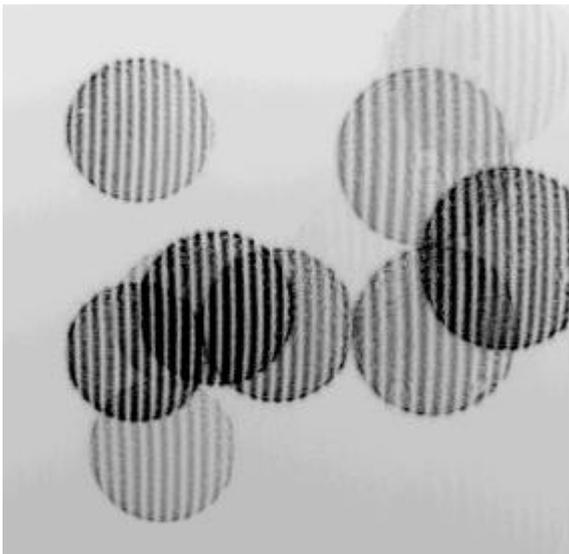
However, the application of the *Mie Scattering Imaging* technique has been limited to homogeneous droplets untill now. On the contrary, in practical systems, homogeneous droplets represent a limit case. The aim of the paper is to establish the theoretical basis and to experimentally test the generalisation of the technique to non-homogeneous spheres. Thus the scattering of radially inhomogeneous droplets was carefully examined in addition to that of homogeneous droplets.

The theoretical analysis of the scattering patterns permits us to conclude that the best angular region to generalise the out-of-focus technique is around $\vartheta=60°$. At this scattering angle the spacing between intensity oscillations is extremely regular and depends only slightly on the refractive index profile. The generalising law for all the refractive indexes is:

$$\Delta\vartheta \, (\vartheta, n(r), D) = 1.129 \, (180° / \alpha) \text{ at } \vartheta=60°.$$

By means of the previous relation, the measure of angular oscillation spacing in out of focus images permits the determination of droplet size within 4%, even if the refractive index is completely unknown. That can represent a powerful tool to study reactive non-isothermal sprays where the hypothesis of homogeneous droplets has to be relaxed. The *Generalised Scattering Image* technique has been successfully applied to homogeneous droplets and droplets in non-stationary vaporisation regime (i.e., with internal variation of refractive index).

Fig.1 Out-of-focus image of 40 mm isopropyl alcohol droplets.

Ragucci R., Cavaliere A. and Massoli P. (1990). Drop sizing by laser light scattering exploiting intensity angular oscillation in the Mie regime" Part. Part. Syst. Charact., 7, pp. 221-225.

1. INTRODUCTION

It is well known that light scattered by homogeneous spheres is characterised by strong angular oscillations. The oscillations, that cause a lot of problems when absolute intensity measurements are carried out, can be used to infer droplet size. In fact, they have an almost uniform angular spacing, $\Delta\vartheta$, which is correlated to the drop diameter by means of the relation $\Delta\vartheta \cong 180°/\alpha$, where α is the size parameter $\alpha = \pi D/\lambda$; D and λ represent, respectively, the diameter of the droplet and the radiation wavelength in the vacuum (Kerker, 1969). The relevant feature is the almost total independence of $\Delta\vartheta$ on the refractive index of the droplet.

On this basis, an optical technique to measure the size of homogeneous droplets was developed (Konig et al., 1986). This approach was initially worked out on the basis of geometrical optics and therefore limited to large spheres and angular regions in forward. The use of the Lorenz-Mie theory permitted the application of the technique to small droplets and to sideward scattering regions too where geometrical optics fails by not foreseeing the presence of surface waves (Ragucci et al., 1990). A correlation between drop diameter and number of oscillations per degree was determined. More relevant, a new optical set-up was developed. The new system, based on a planar imaging of the scattered light, permitted the extension of the technique to 2D-spray analysis. Sideward out-focus images of droplets in a spray were captured. The size of droplets was measured by counting the number of fringes present in each defocused drop image (Ragucci et al., 1990). This approach, that we called *Mie Scattering Imaging*, was subsequently improved. A computer routine to automatically recognise drop images in a spray was developed and the size distribution of droplets in a sparse spray was measured (Glover et al., 1995). More recently the technique was applied with good results to estimate the fuel droplets diameter distribution in a spark ignition engine before ignition (Pajot and Mounaïm-Rousselle, 1998).

However, the application of the *Mie Scattering Imaging* technique has been limited to homogeneous droplets until now. On the contrary, in practical systems, homogeneous droplets represent a limit case. During evaporation-combustion of a droplet, heat is transferred from the surroundings to the droplet surface where it is in part used to vaporise the liquid and in part transmitted inside. A profile of temperature will establish inside the droplet, the surface being the hotter zone. The temperature profile implies a profile of density and, therefore, of the real part of the refractive index. In case of multicomponent droplets, the preferential vaporisation of lighter compounds will generate species concentration profiles and, hence, variations of the real part of the refractive index too. The situation is ulteriorly complicated if new species are generated by chemical transformations of the parent liquid. This will result, typically, in a radial strong increase of the imaginary part of the refractive index. Thus droplets in reactive sprays are expected to present a double radial profile: both for the real and the imaginary part of the refractive index (Massoli, 1998).

The aim of the present paper is to discuss the extension of the *Mie Scattering Imaging* technique to non-homogeneous droplets. This required a systematic theoretical analysis of the scattering by inhomogeneous droplets. The Finely Stratified Sphere Scattering Model (FSSSM) (Li and Massoli, 1994) was used to compute the scattering by radially inhomogeneous spheres. The comprehensive approach, that we call throughout the paper *Generalised Scattering Imaging* (*GSI*), since it is based on other scattering models besides the Mie theory, should permit the sizing of droplets in combustion environment when the hypothesis of homogeneous particles has to be necessarily relaxed. Finally the experimental application of the *GSI* technique to vaporising droplets is discussed. The tests were carried out on streams of calibrated droplets, injected in a controlled high temperature environment operating at different thermal loads. This corresponds to different heat and mass transfer rates and, hence, to different internal temperature and refractive index inhomogeneities.

2. THEORETICAL BACKGROUND

The theoretical basis on which the measure of the angular spacing permits the sizing of homogeneous droplets was already discussed in detail in previous papers for both geometrical optics (Konig et al., 1986) and Mie theory (Ragucci et al., 1990). In this section the attention is dedicated to radially inhomogeneous scatterers. The aim is to furnish the theoretical basis permitting the extension of the sizing technique based on the measurement of the oscillation spacing to objects with a non-homogenous profile of the refractive index. The scattering by spheres with either continuous or discontinuous variation of the refractive index will be analysed.

One of the main problems, from a theoretical point of view, is to discover the angular region where the influence of the refractive index on oscillation spacing, $\Delta\vartheta$, is slightest. In recent papers (Massoli and Calabria, 1999, Massoli, 1999) it was outlined that already in case of homogeneous spheres there is not a constant relation between particle size parameter α and angular spacing of oscillations $\Delta\vartheta$. In fact, the relation $\Delta\vartheta\cong180°/\alpha$ should be considered as a simplification, not valid in the whole angular pattern. For example in the backward region the angular oscillation spacing is $\Delta\vartheta\approx300°/\alpha$ or higher (Massoli, 1998). By using the Lorenz-Mie theory a systematic and detailed analysis about the dependence of $\Delta\vartheta$ on droplet diameter and refractive index in case of homogeneous spheres was carried out. Droplets with diameter between 5 µm and 100 µm and refractive index in the range 1.3 - 1.6 were examined in that theoretical analysis. The large variation of the refractive index used in the computation covered, in practice, almost the totality of liquids in nature. From that computations it appeared that $\Delta\vartheta$ is not constant on the whole angular pattern. In addition, starting from $\vartheta=90°$ the angular spacing showed deep variations that become very large for $\vartheta>120°$. This is due to the complex phenomenology involved in the light scattering process that implies in the side and back scattering regions interference between direct and internally reflected light and surface waves. However, between $\vartheta=40°$ and $\vartheta=80°$, where oscillations are generated by the interference between reflected and refracted light, ϑ is practically constant and the dependence on the refractive index reduces to a minimum at $\vartheta=60°$ (Massoli, 1999).

A preliminary theoretical analysis carried out by Massoli and Calabria (1999) showed that in forward (for a scattering angle between 20° and 60°) the oscillations in the scattering pattern of radially non-homogeneous droplets have spacing almost independent of the refractive index profile. This represented a very promising feature. The *Scattering Imaging* technique developed originally for homogeneous droplets could be applied, with minor modifications, to measure the size of reactive/vaporising droplets in practical combustion systems.

2.1 Radially inhomogeneous spheres with continuous variation of the refractive index

In order to study the extension of the *Scattering Imaging* technique to sprays in non-isothermal regimes, droplets with internal profile of the refractive index are discussed. Droplets in practical combustors vaporise and burn in unsteady conditions presenting, typically, an internal profile of temperature. The surface of droplets will be the hotter zone, with the temperature tending to boiling point, while the central nucleus will be at a lower temperature. This implies a profile of density and, therefore, of the real part, n, of the refractive index that decreases when the droplet surface is approached. In very luminous environments where the amount of heat transmitted by radiative transfer is not negligible, the surface of the droplet acting as a lens can focus the thermal radiation hitting on the surface in an internal region of the droplet. This can generate a hot shell inside the droplet where a temperature which is higher respect to the surface is established.

The refractive index profiles examined in the paper are shown in figure 1. In order to reflect the previous analysis, essentially two different type of refractive index profile were studied. In one case the real part of the refractive index, although with different laws, decreases from the centre to the droplet surface: $dn/dr\leq0$ (profiles *a*, *b*, *d*, *lin*). In the other case n(r) first decreases ($dn/dr\leq0$) and then increases ($dn/dr\geq0$) (profile *b2q*). In all profiles the decrease is smooth. Profiles "*a*" correspond to the initial stage of droplets heating: the droplets are typically characterised by a large homogeneous core with all the variation of the refractive index localised in proximity of the surface. Profiles "*b*" and "*d*" correspond to an advanced stage of the heating when heat is transmitted toward the droplet centre thus increasing the temperature of the inner part too. In order to simulate different classes of liquids, refractive index profiles were varied changing also the initial or the final values. In all profiles the variation of refractive index was large: $\Delta m=0.3$ for profiles with numerical suffix "*1*"; $\Delta m=0.2$ for profiles "*2*", "*3*" and "*lin*"; and $\Delta m=0.1$ for profile "*b2q*". Those large variations of refractive index correspond to large variations in temperature. In fact, typical temperature derivative, $(\delta n/\delta t)_P$, for hydrocarbons is between $4\ 10^{-3}\ °C^{-1}$ and $8\ 10^{-3}\ °C^{-1}$. Thus a variation of 0.1 in refractive index corresponds to a variation in temperature of 250°C and 125°C, respectively.
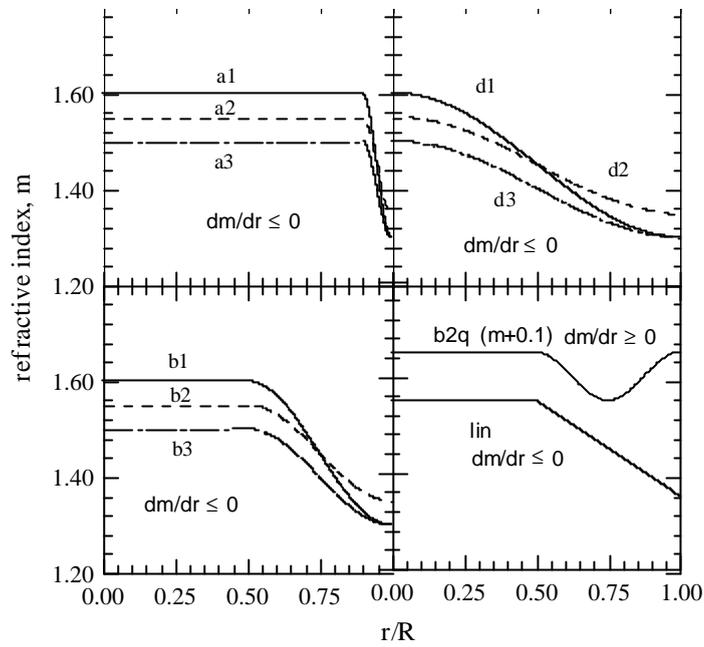
Fig. 1. Refractive index profiles used in the theoretical analysis

Light scattering by radially inhomogeneous droplets was computed by using the finely stratified sphere scattering model, FSSSM (Li and Massoli, 1994). This approach allows the computation of the scattering by stratified spheres with a high number of layers. It was shown that by using the FSSSM with a sufficient number of layers (e.g., 20,000)
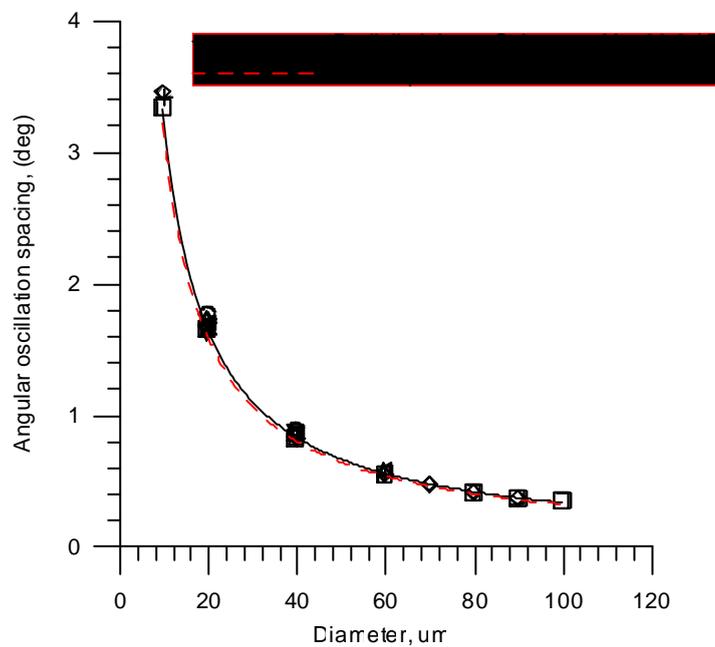

Fig. 2. Angular oscillation spacing vs droplet diameter at $\vartheta = 60°$. Symbols represent calculations relative to radially inhomogeneous droplets whose refractive index profiles are shown in figure 1. For comparison the case of water droplets was reported too.

4

the scattering by spheres with any continuous internal refractive index profile could be calculated with good accuracy (Li and al., 1994).

By using the FSSSM, the angular oscillation periodicity $\Delta\vartheta$ was computed in the case of radially inhomogeneous droplets with the refractive index profiles shown in figure 1 and for droplets whose sizes ranged between 10 µm and 100 µm. For comparison, by using the Lorenz-Mie theory, $\Delta\vartheta$ relative to homogeneous droplets of water was also reported.

The results relative to radially inhomogeneous droplets confirm the preliminary analysis reported in (Massoli and Calabria, 1999). Between $\vartheta=40°$ and $\vartheta=80°$, $\Delta\vartheta$ is practically constant and the dependence on the refractive index reduces to a minimum at $\vartheta=60°$. That is qualified by figure 2 where the dependence of the angular oscillations is plotted in function of the droplet diameter for $\vartheta = 60°$. The best fit of the data gives an equilateral hyperbola with coefficient equal to 33.3: $\Delta\vartheta = 33.3 / D$. That corresponds, after some simple mathematics, to the relation:

$$\Delta\vartheta\,(\vartheta, n(r), D) = 1.129\,(180° / \alpha) \text{ at } \vartheta=60°. \tag{1}$$

For comparison the same computation was performed for homogeneous spheres of water. Also in this case the data is well fitted by an equilateral hyperbola the coefficient of which was equal to 32. The slight dependence of $\Delta\vartheta$ on the refractive index results hence in a sizing uncertainty of about 4%.

3. EXPERIMENTAL SET-UP

The layout of the experimental set-up is shown in figure 3. The second harmonic of a pulsed Nd-YAG laser (Continuum, Power Light) with a maximum frequency repetition of 10 Hz was the light source. The laser pulses are 10 ns short: enough to "freeze" the captured images. The light beam 8 mm in diameter is first expanded by a factor of three via two spherical lenses (f1=50mm and f2=150mm) and then reduced to a vertical sheet (150 µm $\times$ 2 mm in the measuring section) by means of a couple of crossed cylindrical lenses (f3=250 and f4=500mm).
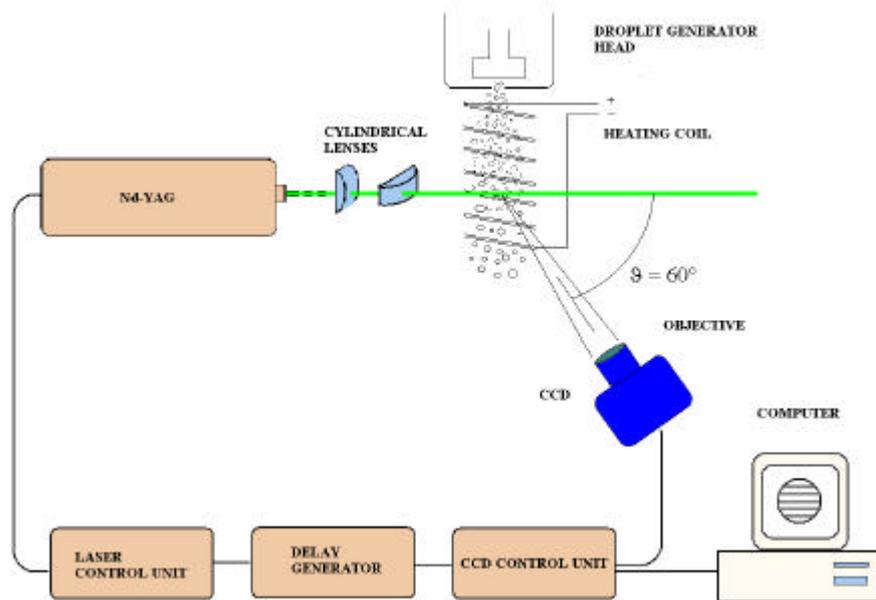

Fig. 3. Experimental set-up

A generator of calibrated droplets (TSI, Vibrating Orifice, mod 3540) was used to produce streams of droplets of known size. By means 20 μm, 35 μm and 50 μm orifices, water and isopropyl alcohol droplets of 45 μm 87 μm and 105 μm were tested in the experiments, respectively. The streams of calibrated droplets were dispersed in a weak airflow (1200 cc/min) and injected in a non-confined coil (6 mm large and 36 mm long) constituted by a ϕ=0.4 mm resistive wire. A dc power supply regulated both in current and voltage was used to power the coil. Tests on droplets were carried out at room temperature (T = 25°C) and at three different coil power rates. The coil entry was positioned at 6 mm from the head of the droplet generator. Coil and generator head were fixed on a small optical bench to form a solid system. They were moved by means a XYZ micropositioner with respect to the laser sheet held at a fixed position.

Droplet images were caught by a 1024x1024 pixels square CCD (Princeton Instruments) equipped with a mechanical shutter. The CCD was placed on a carrier moving on an optical rail. The rail was fixed on a rotating table in order to change the scattering angle. The coarse focusing-defocusing were obtained moving the carrier along the rail. Fine adjustments of the CCD position were achieved by mean a XYZ micropositioner. The centre of the rotating table was in correspondence with the axis of the coil/droplet head generator system. The objective was a 58 mm (Nikkor) upset mounted with an f# between 3.5 and 22. An interference filter peaked at 532 nm, FWHM 10 nm, was mounted in front of the objective. The filter was used to improve the image quality, reducing the background illumination (especially that coming from the incandescent coil in high temperature experiments).

The CCD shutter control signal (SCS) was used to trigger the experiment. The shutter aperture was 100 ms. The rise of the SCS given in correspondence with the shutter opening was delayed by 50 ms by means of a delay generator (Stanford Research Systems, mod. 555) and sent to the Nd-YAG laser to trigger a pulse. Thus a laser pulse was given at the centre of the opening interval of the shutter.

During experiments it is typically necessary to change the f# of the detection optics. It was verified that by changing the f# in a fixed CCD position no variation of the fringe spacing occurred. On the contrary by changing the out-of-focus distance the magnification of the imaged object is changed. Thus, a calibration curve was also determined and the linear dependence of the fringe spacing (as measured on the detector) on the out-of-focus distance was verified.

4. SELECTED RESULTS AND DISCUSSION

Few preliminary tests were carried out in order to both check the reliability and calibrate the experimental apparatus. This series of tests was performed on homogeneous droplets varying the scattering angle and the droplet size. Subsequently experiments were carried out on a graded-index optical fibre. Finally experiments on heated droplets were executed.

4.1 Homogeneous droplets

In a series of preliminary tests the *GSI* technique was applied to homogeneous droplets of different refractive index and size. Isopropyl alcohol and water were utilised in the experiments. In a first series of tests the dependence of the oscillation spacing on the scattering angle was verified. Measurements were carried out between 20° and 150° in steps of 10°. The size of droplets was 45 μm. Figure 4 shows the nice agreement between experimental data and theoretical calculations. The analysis of out of focus images was carried out up to 90°. Besides 90° the analysis was still possible although complicated by the presence of secondary and primary rainbows that generate large variation of oscillation intensity and spacing. In figure 5 out focus images of 45 μm isopropyl alcohol droplets at ϑ=60° and ϑ=140° are reported for comparison.

In a second series of tests the dependence of oscillation spacing at ϑ=60° on the droplets size was tested. Droplets of isopropyl alcohol of 45 μm, 87 μm and 105 μm were used. The experimental data were in good agreement with the theoretical expectation (figure 4). Finally, the slight dependence of the oscillation spacing on the refractive index was also tested. To this aim isopropyl alcohol and water droplets of 45 μm and 47 μm were used. The spacing between oscillations resulted in 0.715° and 0.630°, for isopropyl alcohol and water, respectively.

The comparison between Mie theoretical calculations and the number of fringes and their spacing measured inside out-of-focus images permitted us to infer the exact angular aperture of the detection optics, and more relevant, the absolute calibration of pixels in degrees.
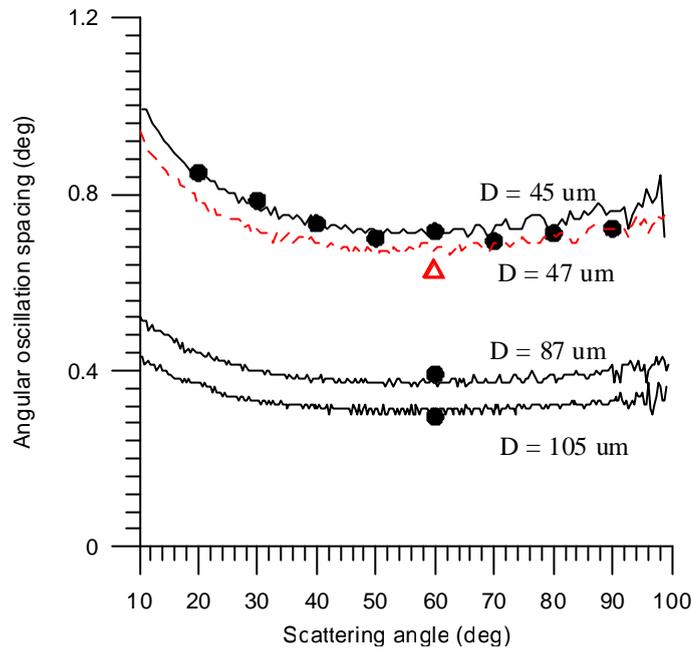

Fig. 4. Angular oscillation spacing in function of the scattering angle for different droplet size. Symbols represent experimental data relative to isopropyl alcohol (circles) and water (triangle). Lines represent theoretical calculations computed by the Mie theory with n = 1.3778 (continuous lines) and n = 1.334 (dashed line), respectively.
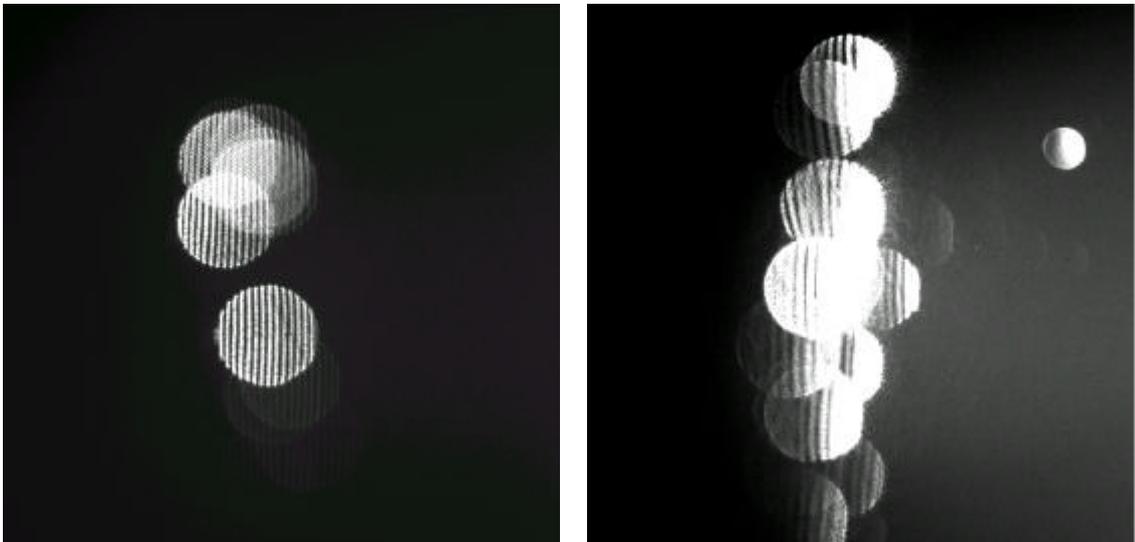

Fig. 5. Out of focus images of 45μm isopropyl alcohol droplets at J = 60° (left) and J = 140° (right)

4.2 A special case: graded-index fibre

In this series of experiments a graded-index optical fibre was used as a scattering reference object. That permitted the testing simultaneously of the reliability of the basis principle of *GSI* technique (i.e., the slight dependence of angular oscillation spacing on refractive index profiles) and also to prove the model of scattering by radially inhomogeneous particles. In fact, the scattering by a cylinder orthogonally illuminated is equivalent to the scattering by a sphere with the same diameter and refractive index as the cylinder. The nominal size of the fibre core and cladding was 50 μm and 125 μm, respectively. The refractive index graded from 1.467 at the centre of the core to 1.45 at the core/cladding interface. The refractive index of the cladding was 1.45. The fibre was fixed vertically to the scattering plane.

The out-of-focus position of the CCD was fixed at +9.5 mm while the scattering angle was varied between 20° and 70°. At each scattering angle the angular spacing between intensity oscillations was measured in out of focus images. In figure 6 the comparison between experimental and theoretical angular oscillation spacing is shown. The agreement is satisfying enough.
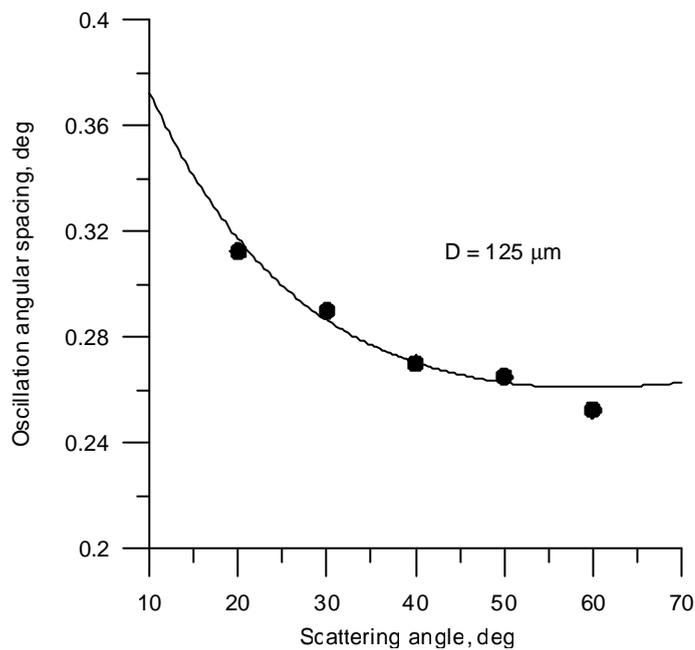

Fig. 6. Angular oscillation spacing in function of the scattering angle for a 50/125 μm graded-index fibre. The line and the circles represent the theoretical calculation and experimental data, respectively.

4.3 Non-homogeneous droplets in evaporating regime

In the last series of experiments the *Generalised Scattering Imaging* technique was applied to measure the size evaporating droplets. Isopropyl alcohol droplets of 45 μm were injected in the resistive coil electrically heated. Three different heating regimes corresponding to different power supply voltages were analysed. The electrical power rates were 30W, 63 W and 110 W, respectively. Table 1 reports the air temperatures measured along the coil axis at different distances from the droplet generator head and for different electrical coil power rates. Air temperatures were measured by a Pt/Pt-Rh ϕ=65 μm exposed junction thermocouple. A thin alumina tube shielded the junction from the thermal radiation emitted by the hot coil.

The droplets were downstream directed with the coil fixed at 6 mm below the exit of the droplet generator. The velocity of droplets was in the range 6 m/s - 10 m/s. By considering the small droplet size and the low air-droplet relative velocity (≈10 m/s) a radially symmetrical heat transfer process can be assumed.

Table 1.

Distance below droplet generator head (mm)	Heat1 P = 30 W (°C)	Heat2 P = 63 W (°C)	Heat3 P = 110 W (°C)
3		302°	
6		432°	
8		451°	
11		489°	
15		354°	
18		323°	
21		312°	
25		292°	
28		292°	
31		281°	
35		292°	
38		292°	
41		312°	
44	143°	302°	460°

As discussed in the theoretical section, angular oscillation spacing measurements permit the sizing of homogeneous and radially inhomogeneous droplets by using the same relation (1). On this basis, out of focus images were caught at the exit of the coil in all three regimes and also in different locations along the coil axis in the intermediate heating condition. The captured images were analysed and the oscillation spacing (in pixels) was measured (figure 7). The spacing was transformed in droplet diameters by using the calibration factor defined in homogeneous droplet experiments (see section 4.1) and finally relation (1).
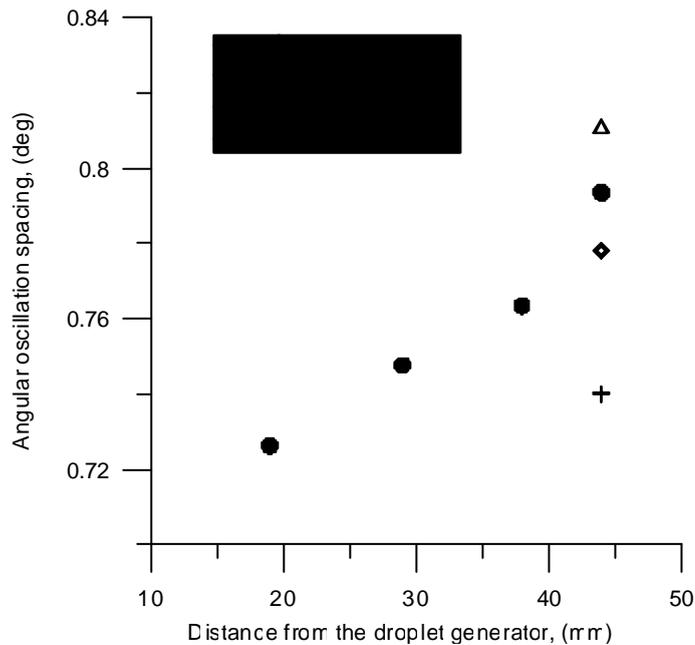

Fig. 7. Angular oscillation spacing measured in out of focus images of isopropyl alcohol droplets at different heating rates and different locations inside the coil. The initial droplet diameter was 45 µm.

9

The inferred droplet diameters are reported in figure 8 in function of the heating regime and of the distance along the coil. Analysing the data corresponding to the intermediate heating condition but at different residence times it is evident that in the first phase of heating, heat is used essentially to warm the droplet. In fact it is interesting to see the increase of the diameter in the first measurement point at 19 mm from the droplet generator head. This should correspond to the liquid volumetric expansion when no evaporation still occurs. Then, a reduction of droplet size is observed increasing the residence time inside the coil (this corresponds to measurements taken in positions more distant from the droplet generator head). At the exit of the coil the size of the droplets was reduced to about 42 μm.
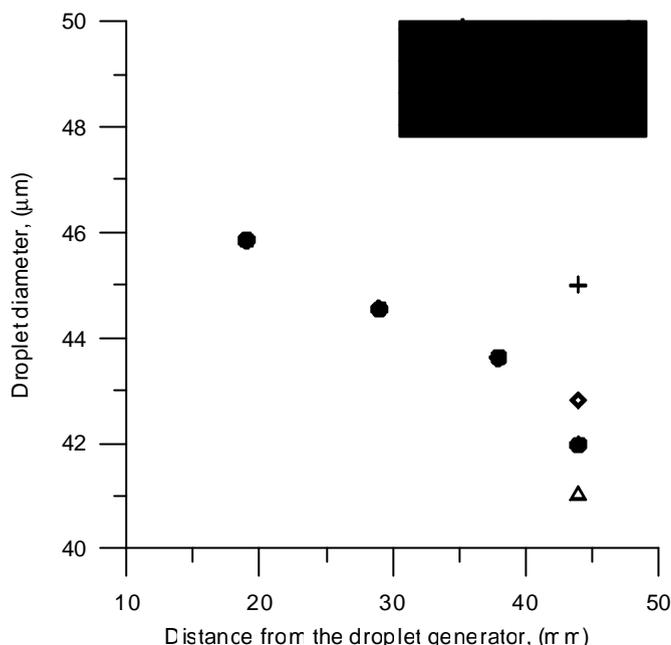

Fig. 8 Mean diameter of isopropyl alcohol droplets measured at different heating rates and different locations inside the coil. The initial droplet diameter was 45 **mm**.

Increasing the heating regime all the processes are faster and vaporisation will be much more significant. On the contrary reducing the thermal load, heat and mass transfer processes are delayed and a limited vaporisation is observed. Thus at the same measurements location, at the exit of the coil, the measured diameters reduced inversely to the thermal load, resulting 42.8 μm, 42 μm and 41 μm for, respectively, 30 W, 63 W and 110 W coil power rates.

5. FINAL REMARKS

A detailed analysis of the scattering by homogeneous and radially inhomogeneous droplets permitted the definition of a common relation by which to infer the size of droplets by measuring the angular spacing of intensity oscillations present in the scattering patterns. Thus the out-of-focus *Mie Scattering Image* technique initially developed for homogeneous droplets is extended to non-homogeneous droplets too. The *Generalised Scattering Image* technique permits the measurement of droplet size within 4% even if their refractive index is completely unknown. A series of experimental tests were carried out on both homogeneous droplets and a radially inhomogeneous fibre to verify the technique. Finally the technique was applied successfully to droplets in the evaporating regime.

REFERENCES

Glover A.R., Skippon S.M. and Doyle R.D. (1995). "*Interferometric laser imaging for droplet sizing: a method for droplet-size measurements in sparse spray systems*", Appl. Opt., 34, pp. 8409-8421.

Kerker M. (1969). "The Scattering of Light and Other Electromagnetic Radiation", Academic Press, New York, p.175.

König G., Anders K., and Frohn A. (1986). "*A new light scatterin technique to measure the diameter of periodically generated moving droplets*", J. Aerosol Sci., 17, pp. 157-167

Li K. and Massoli P. (1994), " *Scattering of electromagnetic-plane waves by radially inhomogeneous spheres: a finely stratifies sphere model* ", Appl. Opt., 33, pp. 501-511.

Li K. Massoli P. and D'Alessio A. (1994), "*Studying inhomogeneities of spherical particles by light scattering*", Part. Part. Syst. Charact., 11, pp. 385-390.

Massoli P. (1998), "*Rainbow refractometry applied to radially inhomogeneous spheres: the critical case of evaporating droplets* ", Appl. Opt., 37, pp. 3227-3235 (1998).

Massoli P. (1999), "*Optical diagnostic of droplets in microgravity*", 5th Intl. Microgravity Combustion Workshop, NASA/CP-1999-208917, May 18th-20th, Cleveland, Ohio.

Massoli P. and Calabria R. (1999), "Sizing of droplets in reactive sprays by Mie scattering imaging", 15th Conf. on Liquid Atomization and Spray Systems, ILASS-Europe, July 5th-7th, Toulouse, France.

Ragucci R., Cavaliere A. and Massoli P. (1990). " *Drop sizing by laser light scattering exploiting intensity angular oscillation in the Mie regime* ", Part. Part. Syst. Charact., 7, pp. 221-225.

Pajot O., Mounaïm-Rousselle C. (1998). "*Droplet sizing by interferometric method based on Mie scattering in an I.C. engine*", 9th Intl. Symp. On Appl. Of Laser Techniques to Fluid Mechanics, July 13th-16th, Lisbon, Portugal.